16th World Conference on Earthquake, 16WCEE 2017

Santiago Chile, January 9th to 13th 2017

Paper N° 3029

Registration Code: S-W1461962097

CORRELATION OF DAMAGE WITH SEISMIC INTENSITY MEASURES FOR DUCTILE CONCRETE BRIDGE COLUMNS IN BRITISH COLUMBIA

S. Ashtari[(1)], C. E. Ventura[(2)]

[(1)] *PhD candidate, department of civil engineering, University of British Columbia, Vancouver, Canada, sepideh.ashtari@civil.ubc.ca*
[(2)] *Professor and director of Earthquake Research Facility, department of civil engineering, University of British Columbia, Vancouver, Canada, ventura@civil.ubc.ca*

Abstract

This study investigates the correlation of a number of ground motion intensity measures with the predicted seismic damage of ductile concrete bridges in British Columbia, Canada. The spectral acceleration at the fundamental period is recommended by bridge codes as the primary intensity measure for selecting and scaling of ground motions records. The suitability of this approach to estimate with confidence the expected damage in bridge columns is investigated in this paper. Three concrete bridge columns with periods of 0.5 s, 1.0 s, and 2.0 s were designed and detailed according to the 2014 Canadian Highway Bridge Design Code (CSA S6-14). Detailed models of the bridge columns with nonlinear displacement-based elements and fiber sections were developed. The columns were subjected to 30 ground motions records, including 10 records from each crustal, subcrustal, and subduction earthquakes, reflecting the complex seismicity of British Columbia. Following the code recommendations, the motions had been selected and linearly scaled individually for each column to match the target spectrum within a period range. Nonlinear time-history analysis was conducted for the 30 records scaled at six hazard levels of 50%, 10%, 5%, 2%, 1%, and 0.5% in 50 years probability of exceedance. To predict the damage to the columns, the maximum drift ratio was employed as the damage indicator. Six discrete damage states were considered for the columns, including minimal damage, yielding of the longitudinal reinforcement bars, spalling of the cover concrete, serviceability limit state of the longitudinal reinforcement bars, crushing of the core concrete, and fracture of the longitudinal reinforcement bars. The analysis results of the 30 records for maximum drift ratios were plotted against each of the candidate intensity measures for all the six hazard levels, and linear correlation of the response with the intensity measures was evaluated. It was observed that among the investigated intensity measures, PGV, and PGD had the strongest positive correlation with the response parameter. Based on this correlation, smaller suites of ground motion records with one third and half of the records in the original suite of 30 records were selected. Predictions for the mean maximum drift ratio and the corresponding damage in the columns were made based on the smaller suites of records, and the results were compared to those from the original suite of records. It was found that the predictions in most cases are reasonably accurate. In some cases the smaller suites may overestimate the response slightly. Employing a smaller number of records for time-history analysis is advantageous for implementing a performance-based design, where a large number of trial and error is required to achieve multiple performance objectives at multiple hazard levels simultaneously. Therefore, the findings of this study could help addressing one of the major challenges ahead of implementing the CSA S6-14 performance-based design approach in practice.

Keywords: correlation; intensity measure; bridge damage; performance-based design, nonlinear time history analysis

1. Introduction

The 2014 Canadian Highway Bridge Design Code [1] requires a performance-based design approach for seismic design of bridges. According to the code, bridges must meet certain performance objectives defined in terms of tolerated structural damage and serviceability objectives, at the three hazard levels of 10%, 5%, and 2% in 50 years probabilities of exceedance. Nonlinear time-history analysis is recommended by the code to assess the damage performance objectives, using minimum of 11 ground motion records. Although using a larger number of records is necessary to assess the final design of bridges, it would be computationally demanding for the trial-and-error-based design process. One way to address this problem is to select a smaller number of records out of the original suite of 11 or more records, which are likely to cause more damage to the bridge, and use this smaller suite for the design process instead of the original suite. It would be most convenient, if the smaller suite of records could be selected without performing any further analysis, and based on ground motion intensity measures only. This would be possible, if there was an adequate correlation between the intensity measures, and the response of bridges, so that the damage could be predicted reasonably by the intensity measures. The main objective of this study is to find a suitable intensity measure, which correlates adequately with damage of ductile concrete bridge columns, and to use this correlation to select a smaller suite of records for non-linear time history analysis, required for the performance-based design process.

First, the ground motion intensity measures, which were examined for this study, are specified. Next, the bridge columns employed in this study, the details of their finite element modelling, and their damage criteria are explained. The next section is dedicated to describing the selection and scaling of the original suite of ground motion records, containing 30 crustal, subcrustal, and subduction motions. Structural analysis details are presented next, followed by the analysis results and discussion of the results.

2. Ground Motion Intensity Measures

The basic task of all ground motion intensity measures is to describe the important characteristics of strong ground motions. Identifying and describing these characteristics lead to better selection and scaling of ground motion records for the purpose of time-history analysis. Traditionally, three main characteristics of amplitude, frequency content, and duration of motions are of interest [2], and many intensity measures have been proposed to describe one or more of these aspects. Nevertheless, due to the complex nature of ground motions, a single factor is incapable of accurately describing all important aspects of ground motions [2, 3].

A number of common and proposed intensity measures were examined in this study, to correlate with damage of ductile concrete bridge columns. The examined parameters are as follows:

1. Amplitude parameters including peak ground acceleration (PGA), peak ground velocity (PGV), and peak ground displacement (PGD).
2. Frequency content parameters including the ratio of peak velocity to peak acceleration (V_{max}/A_{max}).
3. Mixed parameters, which represents more than one aspect of the important ground motion characteristics including Arias intensity, characteristic intensity, Housner spectral intensity, specific energy density, and RMS acceleration and velocity.
4. Proposed parameters by Fajfar et al. [4] and Riddell and Garcia [5]. These parameters consider a combination of peak ground parameters and significant duration of earthquakes.

The definitions of the parameters in the first three numbered items can be found in reference [2].

3. Bridge Column Models

3.1 Description of the bridge columns

To investigate the correlation of the aforementioned intensity measures with the seismic damage of ductile reinforced concrete bridges, simplified single column models were utilized in this study. In ductile substructure reinforced concrete bridges, the substructure elements, such as columns, multiple-column bents, wall-type piers, etc., are designed and detailed to incorporate the seismic damage. In contrast, the superstructure and other elements are designed using the capacity design concept to stay essentially damage free. Also, the focus of this study is on the lateral response of bridges, since in multi-span ductile concrete bridges higher levels of seismic damage typically occur in this direction. The lateral response of these bridges, are dominated primarily by the first mode response. For all the above reasons, it seems justified to use simplified single bridge column models in place of complete models of ductile concrete bridges for the purpose of this study.

Three bridge columns with fundamental periods of 0.5s, 1.0s, and 2.0s were designed and detailed according to the CSA S6-14 [1] force-based design method, with minimum response modification factor of R=3. The three periods cover a relatively wide range of periods for multi-span bridges. The columns were all 2 m in diameter, and are 8.5 m, 14 m, and 21.5 m in height, respectively. The longitudinal reinforcement ratio is 1% in all cases. The weight of the superstructure was assumed to be 200-300 kN/m distributed along the deck. Normal strength concrete with specified compressive strength of 35 MPa was assumed and the grade of reinforcement steel was 400R with minimum specified yield strength of 400 MPa.

3.2 Finite element models

The bridge columns were modelled in SeismoStruct finite element package [6]. Expected material properties for both concrete and reinforcement steel were utilized in the analysis. According to CSA S6-14, Clause 4.7.2 [1], the expected yield strength of reinforcement bars is 1.2 times the minimum specified yield strength, if $R \geq 3$. Also, the expected compressive strength of concrete is 1.25 times the specified compressive strength. Considering material models, Mander et al. constitutive model [7] was utilized for both unconfined and confined concrete with 0.002 m/m strain at the peak value of stress for the unconfined concrete. For the reinforcing steel, Menegotto-Pinto steel model [8], with 0.005 strain hardening parameter, and 0.05 m/m fracture strain was assigned. For other parameters in the material models typical values were assumed.

The columns were modelled with nonlinear displacement-based elements with fiber sections. The size of the elements was selected based on the estimate length of the plastic hinge zone in the columns, and sensitivity analysis on the size of the elements was performed to ensure that localization would not occur in the elements located in the plastic hinge zone. A concentrated mass of 800 tonne was assigned to the top node of each column. This corresponds to mass of a 30 to 40 meter long span deck supported by each column. The associated dead load from the deck was applied as a concentrated gravity force at the top of the columns. The viscous damping was modelled using Rayleigh damping with damping ratio of 3% at the first and second periods of each column. For the boundary condition, it was assumed that the columns are fixed at the base and there is no soil-structure-interaction. The latter assumption is not necessarily realistic for most bridges and soil-structure interaction changes the period of the system, as well as the maximum responses. However, the main goal of this study is to find the trends in how damage in bridge columns are related to various ground motion intensity measures. In future studies, the observed trends should be checked for soil-structure systems as well.

3.3 Damage criteria

Five separate damage states were considered to check the performance of the bridge columns: (1) yielding of the longitudinal reinforcement bars, (2) spalling of the cover concrete, (3) serviceability limit state of the longitudinal reinforcement bars, which corresponds to residual crack width exceeding 1 mm [9], (4) crushing of the core concrete, and (5) fracture of the previously buckled longitudinal reinforcement bars. Strain-based damage criteria were employed to define the damage states of the bridge columns. In that sense, the strains in the fibers are checked against the relevant damage limit states, and if the first fiber reaches the limiting strain values, the program indicates the occurrence of that damage state. The strain limits for the spalling, serviceability limit, and fracture damage states were adopted from the recommended values in Table 4.16 of CSA S6-14 [1]. The tensile yielding strain was calculated as 0.0023 m/m and was used as the strain limit for the yielding damage state. The crushing of core concrete was assumed to occur when compressive strain of the confined concrete fibers reaches -0.01 m/m. This value was calculated from a predictive equation by Mander et al. [7, 10] for the ultimate strain of confined concrete.

Table 1 – Strain-based damage criteria

Damage State	Damage Criteria
Yielding	Reinforcement Strain > 0.0023
Spalling	Concrete Strain < -0.004
Serviceability Limit	Reinforcement Strain > 0.015
Crushing	Concrete Strain < -0.01
Fracture	Reinforcement Strain > 0.05

4. Selection and Scaling of Records

4.1 Description of the site

The British Columbia province located on the west coast of Canada manifests one the most complex seismic regions in the world. Three distinctive sources of earthquakes are active in the region, namely shallow crustal, and deep subcrustal sources, and Cascadia subduction zone. All three sources contribute to the hazard in the region, depending on the fundamental period of the structure, and distance of the site to source.

It is assumed that the bridges under study are all located in the city of Victoria on the southern part of Vancouver Island in British Columbia. The soil site class is assumed to be class C or firm soil, which is the Canada-wide reference ground condition for uniform representation of seismic hazard across the country [11].

4.2 Probabilistic Seismic Hazard Analysis

A probabilistic seismic hazard analysis (PSHA) was performed for the city of Victoria using EZ-FRISK. Formerly, the probabilistic hazard models were available only for the crustal and subcrustal sources, with a deterministic scenario for Cascadia subduction zone [11]. However, the newly proposed probabilistic hazard model for Cascadia subduction zone [12] allows a full PSHA for the region, combining the contributions of all the three sources probabilistically at once. Consequently, uniform hazard spectrum (UHS) of Victoria was obtained for six hazard levels with probability of exceedance of 50%, 10%, 5%, 2%, 1%, and 0.5% in 50 years, corresponding to 72, 475, 975, 2475, 4974, and 9975 year return periods, respectively.

Next, the 2% in 50 years UHS of Victoria was deaggregated in terms of distance and magnitude for each hazard source, and at the periods of 0.5 s, 1.0 s, and 2.0 s, corresponding to the fundamental periods of the three bridge columns. The results of the deaggregation at 1.0 s are tabulated in Table 2 (the results of deaggregation for 0.5 s and 2.0 s periods are not presented here, but were obtained in a similar way). .

Table 2 – Deaggregation of the 2% in 50 years UHS of Victoria at period of 1.0 s

Earthquake Source	Magnitude	Distance (km)
Crustal	6 - 7.5	10 - 50
Subcrustal	6.5 - 7.5	50-100
Subduction	8.5 - 9.5	50-100

4.3 Selection and scaling approach

The procedure for selecting and scaling of ground motion records, follows the recommendation of CSA S6-14 and the code commentary closely, as presented in Clause 4.4.3.6 of the code [1] and C4.4.3.6 of the commentary. The target spectrum for selection and scaling of ground motion records is the UHS for Victoria with 2% in 50 years probability of exceedance, as shown in Fig.1. According to the code, for selecting and scaling the input motions, first a proper period range should be selected. The period range should cover the periods of vibration modes that significantly contribute to the dynamic response of the bridge. The code recommends a period range of $0.2T_1$ to larger of $2T_1$ and 1.5 s, where T_1 is the fundamental period of the bridge. Following the recommendations, the period ranges of interest were determined as 0.1-1.5 s, 0.2-2.0 s, and 0.4-4.0 s for the bridge columns with fundamental periods of 0.5 s, 1.0 s, and 2.0 s, respectively.

For each type of earthquake, i.e. crustal, subcrustal, and subduction, 10 records were selected for time-history analysis, using NGA-West2 database for crustal records, and S2GM online tool for subcrustal and subduction records [13-15]. The selection was made considering the magnitude and distance ranges from hazard deaggregation (Table 2), site soil class, and exclusion of pulse-type near fault motions. The selected records are listed in Table 3, along with the year and location of their corresponding historical event. Referring to the table, it can be observed that many records are from a different geographical location than Victoria. This is due to limitations on the number of the available records from Victoria alone. Nevertheless, the records have been selected based on similarities of soil site class, magnitude, distance, and type of earthquake, and so they can be representative of the earthquakes in Victoria. For this study, only one horizontal component of the records was utilized in time-history analysis. For each bridge column, the records were linearly scaled to match the target spectrum in the period ranges of interest for the column. The scale factors for linear scaling were found by minimizing the square root of the difference between the spectral acceleration response spectrum of each record with the target spectrum, over the period range of scaling. The formulas for calculating the minimum square root of error and scale factors for linear scaling can be found in Reference [16].

Table 3 – Selected ground motion records for time history analysis

Type	Historical Event	Record	Year	Location	No. of Records
Crustal	Chi-Chi	CHY028-E	1999	Taiwan	1
Crustal	Imperial Valley	H-DLT352	1979	California, US	1
Crustal	Kern County	TAF021	1952	California, US	1
Crustal	Kobe	SKI000	1995	Japan	1
Crustal	Landers	ABY090	1992	California, US	1
Crustal	Loma Prieta	A2E090	1989	California, US	1
Crustal	Northridge	UCL360	1994	California, US	1
Crustal	San Fernando	PDL120	1971	California, US	1
Crustal	Superstition Hills	B-IVW090	1987	California, US	1
Crustal	Tabas	BOS-T1	1978	Iran	1
Subcrustal	Geiyo	EHM0150103241528-EW EHM0160103241528-EW	2001	Japan	2
Subcrustal	Miyagi-Oki	IWT0110508161146-NS MYG0060508161146-EW MYG0100508161146-NS MYG0170508161146-NS	2005	Japan	4
Subcrustal	Nisqually	0720c_a-90 1032j_a-58 1416a_a-125 1423c_a-148	2001	Washington, US	4
Subduction	Hokkaido	HKD0770309260450-NS HKD0840309260450-NS HKD0950309260450-EW HKD1090309260450-NS	1952	Japan	4
Subduction	Maule	curico1002271-EW hualane1002271-T stgolaflorida1002271-NS stgopenalolen1002271-EW	2010	Chile	4
Subduction	Tohoku	FKS0071103111446-NS FKS0121103111446-EW	2011	Japan	2

5. Structural Analysis

Nonlinear time-history analysis was performed to calculate the response of the bridge columns at the six hazard levels of 50%, 10%, 5%, 2%, 1%, and 0.5% probabilities of exceedance in 50 years. For each hazard level, the same suite of ground motion records, which had been already selected and scaled for the 2% in 50 years probability of exceedance hazard level, was rescaled for the new hazard level. The scale factor for each hazard level was calculated as $S_a(T_1)_{hazard\ level\ i}/S_a(T_1)_{2\%\ in\ 50\ years}$, in which $S_a(T_1)$ is the spectral acceleration of the UHS for hazard level i at the fundamental period of the bridge column, T_1. The selected horizontal component of the 30 ground motion records were applied to the base of the bridge column models. Effect of geometric nonlinearities, i.e. p-delta effect, was included in the analysis. In total 540 nonlinear time-history analyses were conducted. For each analysis the maximum drift ratio of the top of the bridge columns was extracted as the main response parameter of interest. This is because, for first-mode-response dominated structures, maximum drift ratio is a common index for damage prediction [17]. The analysis was set to stop at the first occurrence of the fracture damage state. This is due to the fact that in most cases, after the first occurrence of the fracture damage state in the models, dynamic instability would initiate, which can be considered as collapse failure in the columns.

To predict the extent of damage in each column, the maximum drift ratios from analysis needed to be checked against the drift ratios corresponding to different damage states of the bridge columns. To find the latter, nonlinear static analysis or pushover analysis was conducted for each of the three columns. The loading pattern for the pushover analysis was a single concentrated horizontal force applied at the top of the bridge columns, and the columns were pushed to the point of failure. The drift ratios corresponding to the first occurrence of each damage state in the columns were considered as the limiting drift ratios to check those damage states. An example of the pushover curve for the 14-meter high bridge column (T_1=1.0 s) is shown in Fig.2. The indicated points on the pushover curve correspond to the first occurrence of the five damage states.

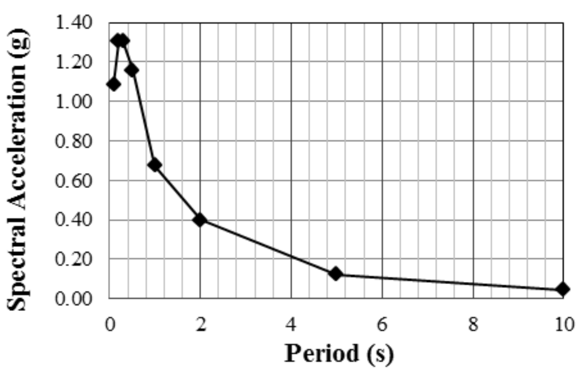

Fig. 1 – Victoria 2015 UHS with 2% in 50 years probability of exceedance

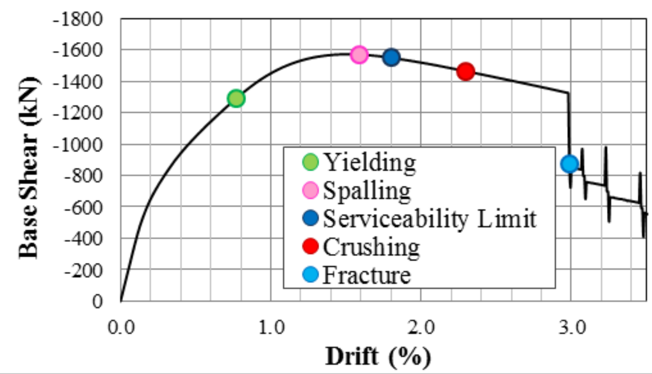

Fig. 2 – Pushover curve for the bridge column with period of 1.0 s

6. Results and Discussion

6.1 Correlation of intensity measures with the response parameter

To check the correlation of damage in bridge columns with the selected ground motion intensity measures, the maximum drift ratios were plotted against each ground motion intensity measure. To do so, the maximum drift ratios for the 30 records scaled at each of the six hazard levels, were plotted against the ground motion intensity measures corresponding to that hazard level. Subsequently, linear correlation coefficient between the intensity measures and the response parameter at each hazard level were calculated. A positive correlation coefficient signifies an increase in the response parameter, and thus the damage in the bridge columns, with an increase in the intensity measure. On the other hand, a zero or a small correlation coefficient indicates that the response parameter is not dependent on that intensity measure. Herein, we are looking for the intensity measures, which demonstrate the strongest positive correlation with the maximum drift ratios. Examples of such plots are given in Fig.3 to Fig.6 for intensity measures PGV, PGD, and V_{max}/A_{max}. The results are shown for only three hazard levels of 50%, 2%, and 0.5 % probabilities of exceedance in 50 years, due to space limitation, and for the sake of clarity of the figures. The following can be observed from the figures:

1. Among the investigated intensity measures PGV, and PGD demonstrated on average higher positive linear correlation with the response parameter, followed by V_{max}/A_{max}, the intensity measure proposed by Fajfar et al., and the Housner spectral intensity.
2. The correlation of the aforementioned intensity measures with the response parameter depends on the hazard level. For lower hazard levels, where the response of the bridge columns is essentially elastic, the linear correlation coefficients are close to zero. The linear correlation tends to increase at the higher hazard levels, and with higher levels of damage.
3. The correlation of the aforementioned intensity measures with the response parameter depends on the fundamental period of the bridge columns.
4. Referring to Fig.3, it can be observed that at higher hazard levels, the linear correlation of PGV with the response parameter is significant and positive for T_1=0.5s, and 1.0s, and becomes negative for T_1=2.0 s.
5. Referring to Fig.5, PGD demonstrates a positive linear correlation with the response parameter. The correlation becomes stronger at larger periods (T_1=2.0 s, and 1.0 s), and decreases for T_1=0.5 s.
6. Referring to Fig.4, V_{max}/A_{max} shows a positive linear correlation with the response parameter, but less strong compared to PGD, and PGV. In this case, the positive correlation tends to improve slightly at larger periods.
7. Fig.6 shows the maximum drift ratio versus PGD of the 1.0 s period column, for each type of earthquakes separately. It is observed that the positive linear correlation at higher hazard levels tends to be stronger for the crustal, and subduction suites compared to the subcrustal suit. This can be explained considering that the response of the bridge column to the subcrustal motions is smaller than the crustal, and subduction motions, at this period, and therefore less damage is incurred to the column by the subcrustal suite. It was observed that for lower levels of damage, the positive linear correlation of the response parameter with the intensity measures is weaker in comparison to higher levels of damage.

It has been already shown in several studies that $S_a(T_1)$, when utilized as the intensity measure to select ground motions, can be both inefficient and insufficient for predicting the response of structures, and the extent of damage [18-22]. Based on the observations of this study, and confirmed by the literature, $S_a(T_1)$ is sufficient at the lower hazard levels, where the response of the bridge columns are essentially elastic. This is the reason why at lower hazard levels, the calculated drift ratios shows minimal variation. However, as the response of the bridge columns moves into the nonlinear range at the higher hazard levels, $S_a(T_1)$ becomes insufficient, and the response becomes dependent on other intensity measures. This is evident referring to the Fig.3 to Fig.6, where the variation of the drift ratios increases considerably at the higher hazard levels.

The observed linear correlation of the response with the investigated intensity measures could be explained theoretically as well. For instance, it is well-known that the response of single-degree-of-freedom systems with very large periods tends to be close to PGD. This is why, at higher levels of damage, where period elongation has occurred, and also for larger fundamental periods, the positive correlation of the response of the bridge columns with PGD is stronger.

6.2 Prediction of damage

Following the main objective of this study, we would like to use the observed correlations to select a smaller suite of records out of the original suite of 30 motions, and examine if using a smaller suite for checking the damage performance objectives is justified. To do so, first the ground motion records should be ranked based on the value of the intensity measure (calculated at the 2% in 50 years probability of exceedance hazard level). Next, the average of the maximum drift ratios for the one third, and half of the records (10 and 20 records) with the highest values of the intensity measures should be calculated. Subsequently, the average drift ratios should be compared to the pushover curves of the columns to predict the damage state of the columns. Finally, the average

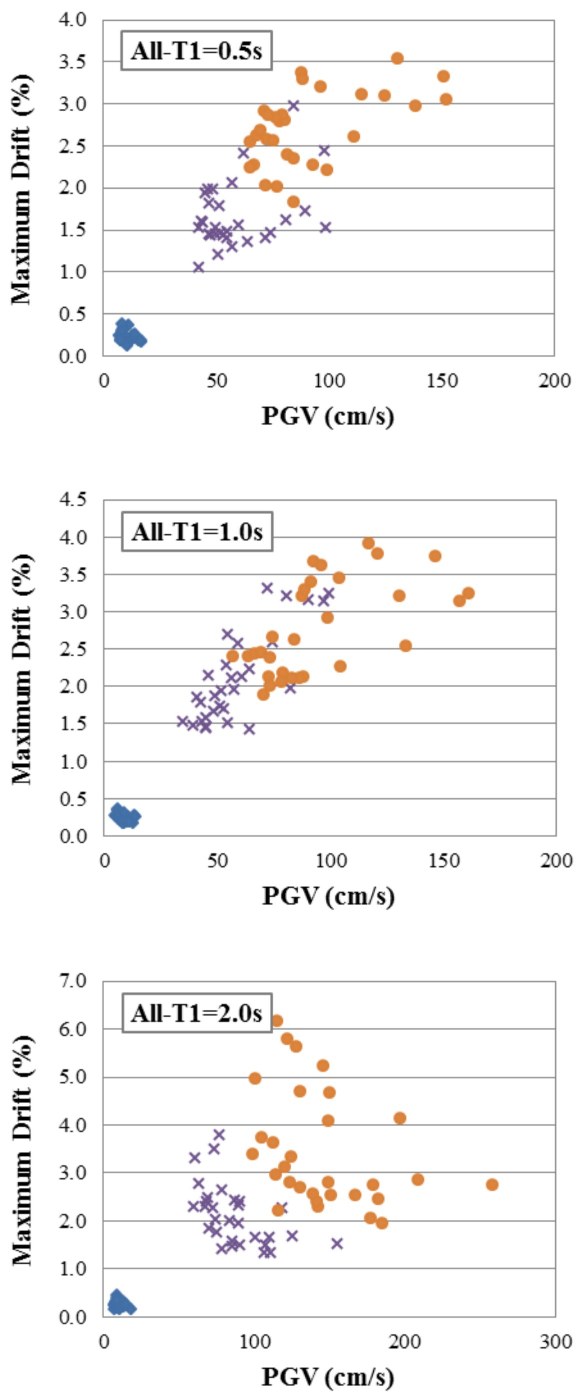

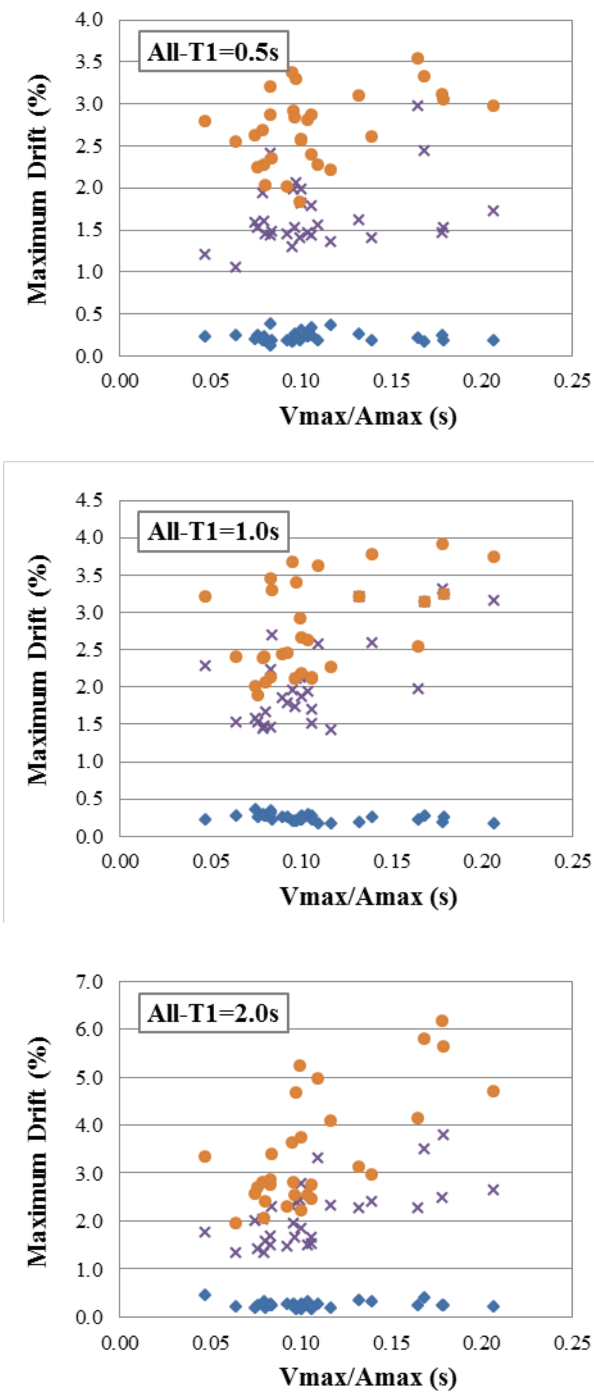

Fig. 3 – Maximum drift ratios versus PGV for the three bridge columns with fundamental periods of 0.5 s, 1.0 s, and 2.0 s

Fig. 4 – Maximum drift ratios versus Vmax/Amax for the three bridge columns with fundamental periods of 0.5 s, 1.0 s, and 2.0 s

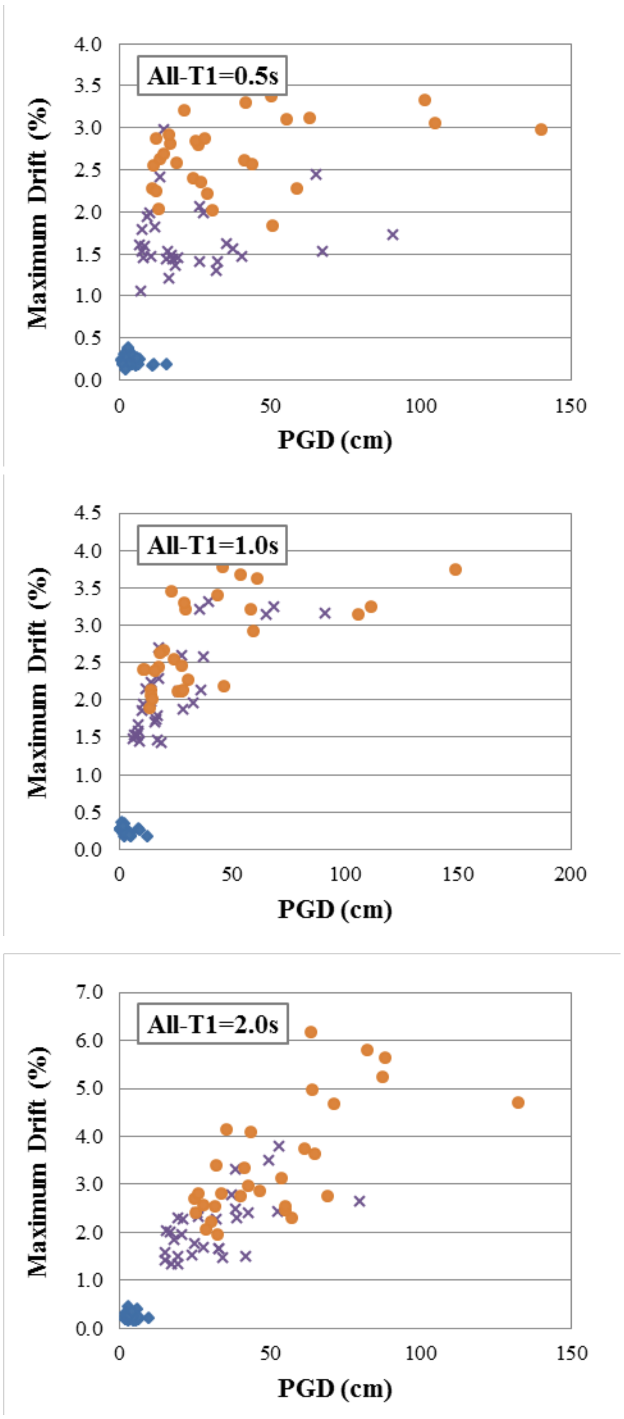

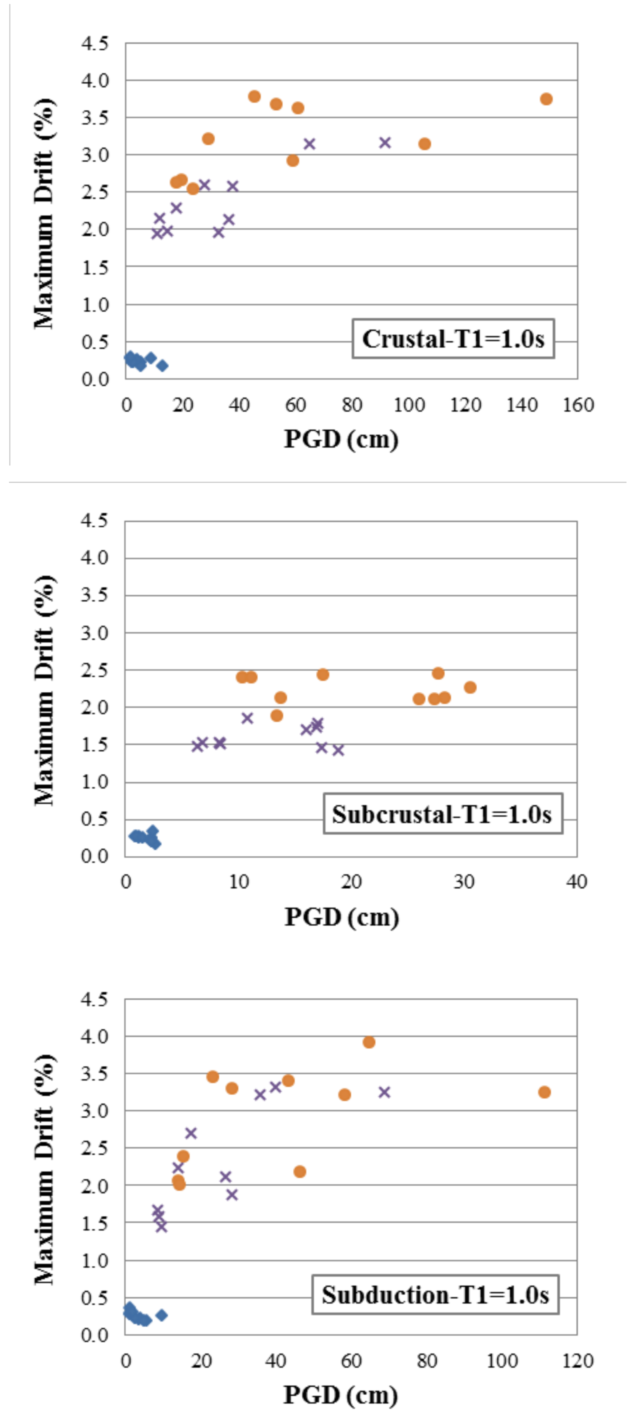

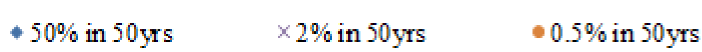

Fig. 5 – Maximum drift ratios versus PGD for the three bridge columns with fundamental periods of 0.5 s, 1.0 s, and 2.0 s

Fig. 6 – Maximum drift ratios versus PGD of the individual earthquake sources for the bridge column with fundamental periods of 1.0 s

Table 4 – Prediction of the damage to the 1.0s period bridge column at different hazard levels using smaller suites of records. PGD was utilized as the intensity measure; μ_n is the average of the maximum drift ratios for n records with the highest PGD values

* Abbreviations: M: minimal damage, Y: yielding, S: spalling, SL: serviceability limit, C: crushing, F: fracture, CR: crustal, SC: subcrustal, SD: subduction

		μ_n	50%/50y	Damage	10%/50y	Damage	5%/50y	Damage	2%/50y	Damage	1%/50y	Damage	0.5%/50y	Damage
T1=1.0 s	CR	μ_3	0.21	M	0.98	Y	2.17	SL	2.96	C	3.29	F	3.49	F
		μ_5	0.21	M	0.95	Y	1.90	SL	2.59	C	3.03	F	3.42	F
		μ_{10}	0.23	M	1.06	Y	1.83	SL	2.39	C	2.83	C	3.19	F
	SC	μ_3	0.26	M	0.86	Y	1.39	Y	1.55	Y	2.03	SL	2.28	SL
		μ_5	0.24	M	0.91	Y	1.36	Y	1.62	S	1.97	SL	2.21	SL
		μ_{10}	0.25	M	0.90	Y	1.31	Y	1.60	S	1.93	SL	2.23	SL
	SD	μ_3	0.21	M	0.86	Y	1.99	SL	3.25	F	3.45	F	3.45	F
		μ_5	0.21	M	0.94	Y	1.74	S	2.75	C	3.06	F	3.18	F
		μ_{10}	0.25	M	0.92	Y	1.57	Y	2.34	C	2.64	C	2.91	C
	All	μ_{10}	0.22	M	0.97	Y	1.88	SL	2.72	C	3.07	F	3.34	F
		μ_{15}	0.22	M	0.96	Y	1.75	S	2.48	C	2.92	C	3.18	F
		μ_{30}	0.25	M	0.96	Y	1.57	Y	2.11	SL	2.47	C	2.77	C

response value and the predicted damage should be compared to those obtained from the original suite of 30 records. Two scenarios are possible:

1. A zero or insignificant linear correlation between the intensity measure and the response parameter at lower hazard levels. In these cases, the values of the response parameter form a small cluster as in Fig.3 and Fig5, or a horizontal line as in Fig.4, and do not depend on the investigated intensity measures ($S_a(T_1)$ is a sufficient intensity measures for these cases). As a result, selecting a smaller suite of one third or half the number of records, whether ranked based on the intensity measure or not, would yield similar average response values as the original suite.

2. There is a positive linear correlation between the intensity measure and the response parameter, at higher hazard levels. In these cases, the records with higher values of the examined intensity measure tend to have larger responses. Therefore, the average of the smaller suite of records selected in this way, tend to have larger to similar average response value as the original suite.

The above scenarios were examined using PGV, PGD, and V_{max}/A_{max} as the intensity measures. Typically it is required to include records from all three types of earthquakes for time-history analysis of bridges in British Columbia. Therefore, it is more reasonable to choose 3 or 5 out of 10 records for each type of earthquake, instead of choosing 10 or 15 out of 30 records, disregarding the type of earthquake. Table 4 includes the comparison of the damage predictions from the smaller suites with the original suite, for the 1.0 s period column. For this case, PGD was employed as the examined intensity measure. In the table, μ_n is the average of the maximum drift ratios for n records with the highest PGD values. For instance, μ_3 is the average of the 3 records out of 10 crustal, subcrustal, or subduction records, with the highest PGD values. Referring to the table, it can be observed that in almost all cases, the smaller suites give reasonable predictions of both the mean response and damage state of the columns. In some cases, they may overestimate the mean response and the corresponding damage. Even so, checking the design with the smaller suites tends to be conservative, and the final design would meet the perceived damage performance objectives, if checked for the original suite of records. Similar observations were made for the other two columns, but due to space limitation, they are not presented here. Readers interested in obtaining the results from the additional studies performed can contact either of the authors at the address shown at the top of the paper.

7. Conclusions

The linear correlation of a number of ground motion intensity measures with the seismic damage of ductile concrete bridge columns in British Columbia has been studied. The examined intensity measures were intended to be utilized to select a smaller suite of records out of the original suite of 11 or more records, for checking performance objectives during the performance-based design trial and error process.

The results of nonlinear time history analysis of three bridge columns with short, medium, and long fundamental periods, demonstrated that PGV, and PGD have reasonable strong positive linear correlation with the maximum drift ratio and damage to the columns. The correlation increases at higher hazard levels, where higher levels of damage incur to the columns. Based on the primary observations of this study, it seems reasonable to employ PGV for shorter period bridge columns (T_1<1.0 s), while using PGD for longer period bridges (T_1>1.0 s), as the intensity measure to select a smaller suite of records out of the original suite of motions.

It was also demonstrated that it is possible to employ the aforementioned intensity measures to select a suite of one third or half the size of the original suite of records, which would still yield a reasonable prediction of the mean response and the corresponding damage to the bridge columns. Using a smaller number of records for the design trial and error process is very advantageous in terms of time and computational effort for performance-based design of bridges, where multiple performance-objectives at multiple hazard levels must be met simultaneously. However, it should be recognized that the conclusions of this study are based on primary observations for a limited number of bridge columns. Further studies are needed to confirm the applicability of these outcomes to performance-based design of all ductile concrete bridges.

8. Acknowledgements

This research project is financially supported by the University of British Columbia, through doctoral fellowship award. The authors greatly appreciate the help of Prof. Liam Finn, and Prof. Ricardo Foschi from UBC, for providing invaluable feedbacks and comments on the paper. They would also like to thank Dr. Armin Bebamzadeh from UBC, for helping with the selection of subcrustal and subduction motions, used in this study.

9. References

[1] CSA (2014): S6-14 Canadian Highway Bridge Design Code.

[2] Kramer SL (1995): *Geotechnical Earthquake Engineering*. Pearson Education, 1st edition.

[3] Jennings PC (1985): Ground motion parameters that influence structural damage. *Strong Ground Motion Simulation and Engineering Application*, EERI Publication 85-02, Earthquake Engineering Research Institute, Berkeley, USA.

[4] Fajfar P, Tomaz V, Matej F (1990): A measure of earthquake motion capacity to damage medium-period structures. *Soil Dynamics and Earthquake Engineering*, **9** (5), 236-242.

[5] Riddell R, Garcia JE (2001): Hysteretic energy spectrum and damage control. *Earthquake Engineering and Structural Dynamics*, **30**, 1791-1816.

[6] SEiSMOSOFT (2015): SeismoStruct. http://www.seismosoft.com/seismomatch.

[7] Mander JP, Priestley MJN, Park R (1988): Theoretical stress-strain model for confined concrete. *Journal of Structural Engineering*, **114**(8), 1804-1826.

[8] Menegotto M, Pinto E (1973): Methods of analysis for cyclically loaded reinforced concrete plane frames including changes in geometry and non-elastic behaviour of elements under combined normal force and bending. *IABSE Symposium*.

[9] Kowalsky MJ (2000): Deformation limit states for circular reinforced concrete bridge columns. *Journal of Structural Engineering*, **126**(8), 869-878.

[10] Hewes JT, Priestley MJN (2002): Seismic design and performance of precast concrete segmental bridge columns. *Rep. No. UCSD/SSRP-2001/25*, University of California, San Diego.

[11] Adams J, Halchuk S (2003): Fourth generation of hazard maps of Canada: Values for over 650 Canadian localities intended for the 2005 National Building Code of Canada. *Open File 4459*, Geological Survey of Canada.

[12] Halchuk S, Allen TI, Adams J, Rogers GC (2014): Fifth generation seismic hazard model input files as proposed to produce values for the 2015 National Building Code of Canada. *Open File 7576*, Geological Survey of Canada.

[13] Pacific Earthquake Engineering Research Center (2013): PEER NGA-West2 ground motion database for shallow crustal earthquakes in active tectonic regimes. http://ngawest2.berkeley.edu/.

[14] Selection and Scaling of Ground Motions (2014): S^{2}GM. http://s2gm.hpcperformancedesign.com/.

[15] Bebamzadeh A, Ventura C (2015): New performance-based design tools developed at University of British Columbia. *2015 LATBSDC conference*. Los Angeles, California, US.

[16] Pacific Earthquake Engineering Research Center (2010) Technical report for the PEER Ground Motion Database web application. http://ngawest2.berkeley.edu/Technical_Report.pdf.

[17] Cordova PP, Deierlein GG, Mehanny SSF, Cornell CA (2001): Development of a two-parameter seismic intensity measure and probabilistic assessment procedure. *The Second US-Japan Workshop on Performance-Based Earthquake Engineering Methodology for Reinforced Concrete Building Structures*. 2000.

[18] Baker J, Cornell CA (2005): A vector-valued ground motion intensity measure consisting of spectral acceleration and epsilon. *Earthquake Engineering and Structural Dynamics*, **34** (10), 1193-1217.

[19] Baker J, Cornell CA (2006): Spectral shape, epsilon and record selection. *Earthquake Engineering and Structural Dynamics*, **35** (9), 1077-1095.

[20] Tothong P, Luco N (2007): Probabilistic seismic demand analysis using advanced ground motion intensity measures. *Earthquake Engineering and Structural Dynamics*, **36** (13), 311-321.

[21] Luco N, Bazzuro P (2007): Does amplitude scaling of ground motion records result in biased nonlinear structural drift responses?. *Earthquake Engineering and Structural Dynamics*, **36** (13), 1813-1835.

[22] Huang YN, Whittaker AS, Luco N, Hamburger R (2009): Scaling earthquake ground motions for performance-based assessment of buildings. *Journal of Structural Engineering*, 10.1061/ (ASCE) ST.1943-541X.0000155, 311-321.